# The potential of spaceborne dual-wavelength radar to make global measurements of cirrus clouds

ROBIN J. HOGAN* AND ANTHONY J. ILLINGWORTH

*Department of Meteorology, University of Reading, UK*

J. Atmos. Oceanic Tech., 1999, **16**, 518–531

ABSTRACT

Spaceborne millimeter-wave radar has been identified as a possible instrument to make global measurements in ice clouds, which have an important but poorly-understood role in the earth's radiation budget. In this paper we explore the potential of a dual-frequency spaceborne radar to estimate crystal size in cirrus clouds, and hence determine ice water content and short-wave extinction coefficient more accurately than would be possible using a single radar. Calculations show that gaseous attenuation is not a serious problem for a nadir-pointing radar measuring down to cirrus altitudes at frequencies between 35 and 215 GHz, provided the frequencies are chosen to lie in the window regions of the atmospheric absorption spectrum. This enables the significant benefits to be exploited of using frequencies too high to be operated from the ground. Radar reflectivity at 35, 79, 94, 140 and 215 GHz has been calculated from aircraft ice-particle size spectra obtained during the EUCREX and CEPEX campaigns, and it is shown that overall the most promising dual-wavelength combination for measuring crystal size and ice water content is 79 and 215 GHz. For a minimum radar sensitivity of −30 dBZ, this combination can measure ice water content and median volume diameter with errors of between 10 and 30% when the reflectivity is greater than −15 dBZ (equivalent to an ice water content of around 0.015 g m$^{-3}$). If only a single wavelength radar were affordable then for estimating ice water content 215 GHz would be the preferred choice. Since the two radars would be likely to use the same antenna, we also consider the effect of cloud inhomogeneities to introduce a random error into the reflectivity ratio because of the different beamwidths at each frequency. It is found, using data from the cloud radars at Chilbolton, England, that this is more than 0.2 dB for frequency pairings which include 35 GHz, but for all other combinations is less than 0.1 dB, which is comparable to the other errors in the system and much smaller than the typical values being measured. Non-spherical crystals are shown to have a significant effect on the size measured by a nadir pointing dual-wavelength radar, but we present evidence that this can be largely eliminated by viewing at 45° from nadir.

## 1. Introduction

The importance of ice clouds in the climate system is well recognised (Stephens et al. 1990), and attention recently has focussed on ways to globally measure the radiative properties and water content of these clouds using active instruments from space. Brown et al. (1995) analysed aircraft cloud probe data taken during EUCREX (the European Cloud Radiation Experiment) and CEPEX (the Central Equatorial Pacific Experiment) to determine how accurately a single 94 GHz radar could measure ice water content (IWC). They found that from radar reflectivity factor alone it should be possible to measure IWC with a standard error of +85% and −45% for IWC greater than 0.01 g m$^{-3}$, but that if the median size of the ice crystal distribution could be derived using other instruments on board the satellite, then the error would be reduced to +50% and −35%. For IWC=0.001 g m$^{-3}$ these errors increase to between +140% and −40% when size is unknown, and +80% and −45% when size is known. The remaining error when size is known is due entirely to deviations of the crystal size distribution from exponential. They concluded that if no size information was available then the data from the radar would still provide a useful constraint for climate models, and with the proposed sensitivity threshold of −30 dBZ all but a few percent of radiatively significant clouds would be detected. A similar study was carried out by Atlas et al. (1995) using aircraft data from FIRE (the First ISCCP Regional Experiment), although from broadly comparable results they concluded that without size available, any estimate of IWC would be too inaccurate to be any use for models, and also that a significant fraction of radiatively important clouds would be missed with a minimum sensitivity of −30 dBZ.

The important question of how additional instruments aboard the satellite could be used to derive size has yet to be fully addressed. It was demonstrated by Intrieri et al. (1993) that crystal size can be retrieved using ground-based radar and infrared lidar due to the very different diameter-dependence of the backscattered power. They used a $CO_2$ lidar (10.6 $\mu$m), but gas lidars tend to be large instruments and generally unsuited to use from space. In theory a visible lidar should be able to serve the same purpose, but this has yet to be demonstrated from the ground. Additionally, reliable techniques to correct for the strong multiple scattering and attenuation at lidar wavelengths need to be developed before size measurement from space using this method could expect any success.

One possible alternative is to use two radars of differ-

*Corresponding author address: Department of Meteorology, PO Box 243, Earley Gate, Reading RG6 6BB, United Kingdom. E-mail: r.j.hogan@reading.ac.uk.

ent frequencies, with the higher frequency scattering sufficiently outside the Rayleigh regime that as crystal size increases, reflectivity factor measured at this frequency ($Z_{\text{high}}$) falls below that at the lower frequency ($Z_{\text{low}}$), and the dual-wavelength ratio, defined as

$$\text{DWR} = 10\log_{10}\left(\frac{Z_{\text{low}}}{Z_{\text{high}}}\right) \text{ dB}, \tag{1}$$

rises above 0 dB and is directly related to crystal size. This principle was first suggested by Matrosov (1993), and was demonstrated using ground-based 35 and 94 GHz radars by Hogan et al. (2000), although DWR was observed to rise to only 8 dB, and random error in DWR at low signal-to-noise ratios prevented size estimation in a significant fraction of detected cloud.

This problem would be much reduced by the use of higher frequencies. Gaseous attenuation normally precludes the use of frequencies higher than around 94 GHz for ground-based cirrus observations, but from space the attenuation is reduced to an acceptable level (see Section 4). The advantages of higher frequencies are:

1. A large increase in DWR for a given mean crystal size, enabling more accurate size retrieval and the ability to measure down to smaller sizes;

2. Higher sensitivity: in the Rayleigh regime, reflectivity increases as the fourth power of frequency for a fixed antenna size, although this is partially countered by increased thermal noise and reduced power output;

3. A smaller footprint;

4. For single frequency radars, the use of higher frequencies results in a closer correlation between IWC and $Z$ (see Section b).

The frequencies we shall consider in this paper are 35, 79, 94, 140 and 215 GHz, chosen because they lie in the window regions of the atmospheric absorption spectrum. 35 and 94 GHz radars have been used in cloud research for over 10 years, but of the other frequencies the authors are aware of only a single 215 GHz radar in existence (Mead et al. 1989). This ground-based radar uses a similar transmitting tube to the 94 GHz radar of Lhermitte (1988), but the power output is less by 12.2 dB because of the higher operating frequency, which largely offsets the 14.4 dB increase in sensitivity due to increased scattering efficiency. The radar is restricted to probing low clouds because of the strong water-vapor attenuation in the boundary layer.

Radar reflectivity at these five frequencies, and the relevant microphysical parameters, have been calculated from the EUCREX and CEPEX datasets. Firstly the accuracy of simple estimates of IWC and visible extinction coefficient ($\beta_{\text{vis}}$) from radar reflectivity alone are calculated for each wavelength. Then we compute the improved accuracy of these parameters using various combinations of these frequencies, and also the accuracy of retrievals of median volume diameter $D_0$. Lastly the effect of minimum detectability thresholds of both $-30$ and $-40$ dBZ is determined, by adding the appropriate random noise to DWR and recalculating the retrieved cloud parameters.

The magnitude of the attenuation by atmospheric gases is calculated for a number of standard atmospheres in Section 4, and is found to be acceptable down to the melting level, even at 215 GHz. We also calculate the attenuation by the ice crystals themselves for the EUCREX and CEPEX data. In Section 5 we estimate to what extent the different beamwidths of a dual-wavelength radar using the same antenna could cause errors in DWR while probing inhomogeneous cloud. This is achieved by using real cloud radar data to obtain the amplitude of reflectivity fluctuations at various spatial scales, and then simulating two-dimensional cloud fields with the same spectral properties. This method is also used to explore the feasibility of mounting the two radars of a dual-wavelength system on separate satellites in very close orbits. Other considerations such as calibration and the effects of non-spherical crystals are considered in Section 6.

## 2. Theory

### *a. Cloud parameters*

The most basic cloud parameters required by radiation schemes are the short-wave volume extinction coefficient $\beta_{\text{vis}}$ and the infrared volume absorption coefficient $\beta_{\text{ir}}$. It is common to assume in both the visible and the infrared that ice crystals are large compared with the wavelength, and hence make the geometric optics approximation:

$$\beta_{\text{vis}} \simeq 2\int_0^\infty \mathsf{A}(D)\, n(D)\, dD \tag{2}$$

$$\beta_{\text{ir}} \simeq \int_0^\infty \mathsf{A}(D)\, n(D)\, dD \tag{3}$$

where $\mathsf{A}(D)$ is the particle cross-sectional area as a function of diameter $D$, and $n(D)$ is the crystal number concentration per unit diameter.

For direct comparison with atmospheric models it is necessary for remote sensing techniques to measure ice water content (IWC). To calculate this from aircraft data, which consist of particle concentration in a number of size bins, we must prescribe a shape and density. For simplicity we assume spheres, and from the mass-diameter relationship of Brown and Francis (1995), density $\rho$ is derived as:

$$\rho = 0.07 D^{-1.1} \text{ g cm}^{-3} \tag{4}$$

to a maximum of 0.917 g cm$^{-3}$, where the diameter $D$ is in millimeters. Brown and Francis found that their relationship maximised the agreement between the bulk measure of IWC from the Total Water Probe (Brown 1993)

and that calculated from size spectra. This density function is also used in the calculation of radar reflectivity.

To assess the ability of the dual-wavelength method to estimate size, the median diameter of the volume-weighted size distribution, $D_0$, is used. This is often used as a parameter in idealised size distributions.

*b. Radar parameters*

Radars measure effective radar reflectivity, which for spherical particles at frequency $f$ is given by

$$Z_f = \int_0^\infty \frac{|K(\rho)|^2}{0.93} n(D)\, D^6 \gamma_f(D)\, dD \qquad (5)$$

where $\gamma_f$ is the ratio of Mie to Rayleigh backscatter. The parameter $K$ is given by

$$K = \frac{\epsilon - 1}{\epsilon + 2} \qquad (6)$$

where $\epsilon$ is the complex dielectric constant of the ice-air mixture. The dielectric constant of solid ice ($\epsilon_s$) is calculated using the empirical expression of Liebe et al. (1989), and given the ice fraction of the crystal lattice ($f_i$), $\epsilon$ can be calculated using the formula of Maxwell-Garnet (1904), as modified by Meneghini and Liao (1996):

$$\epsilon = \frac{(1 - f_i)\epsilon_a + f_i \alpha \epsilon_s}{(1 - f_i) + f_i \alpha} \qquad (7)$$

where

$$\alpha = \frac{2\epsilon_a}{\epsilon_s - \epsilon_a}\left[\frac{\epsilon_s}{\epsilon_s - \epsilon_a} \ln\left(\frac{\epsilon_s}{\epsilon_a}\right) - 1\right] \qquad (8)$$

and the dielectric constant of air ($\epsilon_a$) is taken to be unity. It turns out that $|K|^2$ is approximately proportional to the square of density, and is virtually independent of frequency between 35 and 215 GHz. Because the radar measure of $Z$ has no a priori knowledge of the phase of the target, and to enable comparison of different wavelengths, the factor 0.93 is present in (5) to make reflectivity factor relative to liquid water at centimeter wavelengths. Clearly $Z$ is not directly proportional to any cloud parameter of interest, so it is necessary to derive empirical relationships from real data.

For dual-frequency radar, six combinations of frequencies are considered: 35/94, 35/140, 35/215, 79/140, 79/215 and 140/215 GHz. To illustrate the typical magnitude of DWR for each, Fig. 1 shows DWR as a function of $D_0$ for exponential distributions of spherical crystals.

*c. Accuracy of radar parameters*

A crucial concern for dual-wavelength radars is the extent to which various factors might introduce error into DWR. The problem of different beamwidths is explored in Section a, and that of calibration in Section b. Here we consider the random error in reflectivity measurements at low signal-to-noise ratios. For a single wavelength radar this is not usually of great importance, but for dual-wavelength radar it is what determines the lower size limit for the use of DWR.

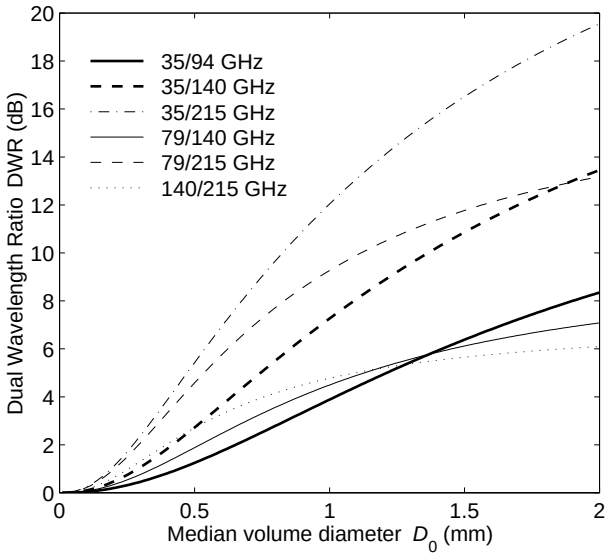


FIG. 1: Dual-wavelength ratio as a function of median volume diameter for an exponential distribution.

Throughout this paper we adopt the retrieval strategy suggested by Illingworth et al. (1997). They considered a nadir-pointing 79 or 94 GHz radar of the conventional pulsed type in a 500 km high orbit, and showed that at this altitude the maximum allowable Pulse Repetition Frequency to avoid mirror image cloud returns is 2830 Hz. In general, the noise component of the measured echo can be considered statistically independent every pulse, and for the cloud echo the decorrelation time is approximately equal to the reciprocal of the Doppler bandwidth within the mainbeam of the antenna. In the case we are considering the decorrelation time is around 0.1 ms, so we can consider all pulses to be independent.

It can be shown that for a radar with a noise-equivalent reflectivity (for a single pulse) $N$, the standard error of a reflectivity measurement averaged over $M_I$ independent pulses is given approximately by

$$\Delta Z \simeq \frac{4.343}{\sqrt{M_I}} \left(1 + 10^{0.1(N[\mathrm{dBZ}] - Z[\mathrm{dBZ}])}\right) \ \mathrm{dB}. \qquad (9)$$

Hence for a 1 second dwell (7 km along-track averaging), $M_I = 2830$, and in the limit of large signal-to-noise ratio, $\Delta Z \to 0.082$ dB. More information on the accuracy of $Z$ measurements can be found in Doviak and Zrnić (1993).

It is necessary to define a threshold reflectivity for cloud detection. In Illingworth et al. (1997) the cloud was deemed detectable if the radiometric resolution, defined

as

$$\gamma = 1 + \frac{1}{\sqrt{M_1}}\left(1 + 10^{0.1(N[\mathrm{dBZ}] - Z[\mathrm{dBZ}])}\right), \qquad (10)$$

was less than 1.5. This is equivalent to setting the maximum allowable $\Delta Z$ to 2.17 dB, or specifying that in clear skies with only (normally-distributed) noise being detected, only 2.3% of the pixels would anomalously register as cloud. These could then be almost completely eliminated by rejecting all low reflectivity pixels not adjacent to any other pixel. At both frequencies of a dual-frequency system we calculate $\Delta Z$ as a function of reflectivity and minimum detectable reflectivity, and from this the error in DWR:

$$\Delta\mathrm{DWR} = \left(\Delta Z_{\mathrm{high}}^2 + \Delta Z_{\mathrm{low}}^2\right)^{\frac{1}{2}} \ \mathrm{dB}. \qquad (11)$$

Hence in the limit of large signal-to-noise ratio, $\Delta\mathrm{DWR} \rightarrow 0.12\,\mathrm{dB}$. It was stated in Illingworth et al. (1997) that with current technology a 79 or 94 GHz spaceborne radar could be built to have a minimum detectable reflectivity of $-30$ dBZ in this retrieval scenario.

## 3. Accuracy of cloud parameters derived by spaceborne radar

### *a. Brief description of the aircraft data*

The data used in this section comprise mid-latitude measurements from EUCREX and tropical measurements from CEPEX. They are the same as those used by Brown et al. (1995), but with a few additional mid-latitude flights which have been grouped together with the existing EUCREX data. See Brown et al. for more information. The EUCREX dataset consisted of over 10 000 5-second averaged size spectra, discretised into 50 bins ranging from 25 to 6400 $\mu$m in diameter. The flights were by the UK Meteorological Office C-130 aircraft and took place in September and October 1993. The CEPEX data comprised a similar number of 10-second averaged size spectra in 28 bins between 45 and 2700 $\mu$m. The aircraft was a Learjet of Aeromet Inc. and the flights occured in March and early April 1993. Observations at temperatures above $-20^{\circ}$C were rejected because of the possibility of contamination from supercooled water droplets which would have biased the results.

Radar reflectivity at 35, 79, 94, 140 and 215 GHz was calculated from the spectra using Mie theory, along with the parameters IWC, $\beta_{\mathrm{vis}}$ and $D_0$. Histograms of the IWC observations are shown in Fig. 2.

### *b. Accuracy of single wavelength measurements*

Firstly the accuracy of simple empirical estimates of IWC from radar reflectivity were calculated for each wavelength as a function of IWC. The parameters of a least squares fit regression between $Z$ and $\log_{10}(\mathrm{IWC})$ were computed, and are given in Table 1. At higher frequencies the effect of increased Mie scattering is to increase the slope of the lines of best fit. The small difference between the coefficients given for 94 GHz and those in Brown et al. (1995) are due mainly to the fact that they only performed regressions on part of the datasets in order to test their representativeness, and to explore how systematic differences in IWC–$Z$ relationships from cloud to cloud could affect the accuracy of retrievals.

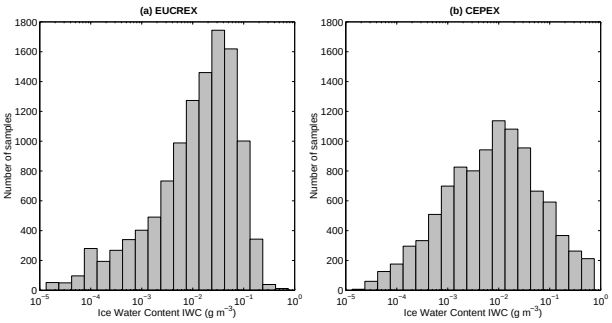


FIG. 2: Histograms of the IWC observations for the EUCREX and CEPEX datasets.

| | frequency | $a$ | $b$ |
|---|---|---|---|
| EUCREX | 35 GHz | 0.0619 | −1.078 |
| | 79 GHz | 0.0691 | −0.888 |
| | 94 GHz | 0.0706 | −0.846 |
| | 140 GHz | 0.0749 | −0.713 |
| | 215 GHz | 0.0820 | −0.461 |
| CEPEX | 35 GHz | 0.0617 | −0.899 |
| | 79 GHz | 0.0638 | −0.834 |
| | 94 GHz | 0.0647 | −0.805 |
| | 140 GHz | 0.0677 | −0.700 |
| | 215 GHz | 0.0734 | −0.489 |

TABLE 1: Coefficients of the least squares fit $\log_{10}(\mathrm{IWC}) = aZ + b$, where $Z$ is in dBZ and IWC is in g m$^{-3}$.

However, for determining the errors in IWC, the fit used was an interpolation between the mean of $\log_{10}(\mathrm{IWC})$ in each 5 dB range of $Z$, which led to greater accuracy in the thickest and hence most radiatively important clouds.

Figure 3 shows the fractional standard error in IWC estimated from $Z$, as a function of IWC for the five frequencies. Fractional standard error is defined simply as the standard error of the natural logarithm. For small relative errors this is approximately equal to the standard error divided by the mean. It can be seen that accuracy improves with increased frequency. This is for the simple reason that the Mie scattering regime represents a transition between the Rayleigh scattering regime (where backscattered power is proportional to $D^6$) and the geometric optics regime (where backscattered power is proportional to $D^2$). Hence the return from frequencies which are backscattering further into the Mie regime has a

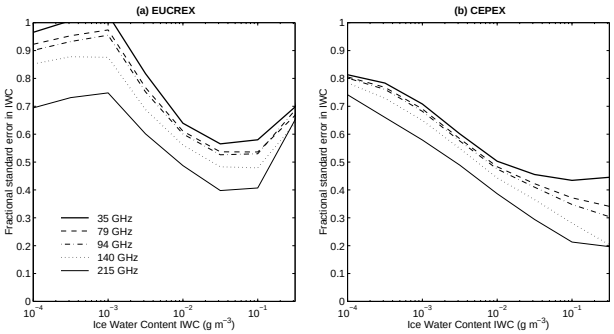


FIG. 3: Error in ice water content estimated by radar reflectivity at five frequencies for the EUCREX and CEPEX datasets.

| | frequency | $a$ | $b$ |
|---|---|---|---|
| EUCREX | 35 GHz | 0.0607 | −2.493 |
| | 79 GHz | 0.0677 | −2.309 |
| | 94 GHz | 0.0691 | −2.268 |
| | 140 GHz | 0.0732 | −2.139 |
| | 215 GHz | 0.0800 | −1.894 |
| CEPEX | 35 GHz | 0.0584 | −2.306 |
| | 79 GHz | 0.0603 | −2.244 |
| | 94 GHz | 0.0611 | −2.217 |
| | 140 GHz | 0.0640 | −2.117 |
| | 215 GHz | 0.0694 | −1.917 |

TABLE 2: Coefficients of the least squares fit $\log_{10}(\beta_{\rm vis}) = aZ + b$, where $Z$ is in dBZ and $\beta_{\rm vis}$ is in m$^{-1}$.

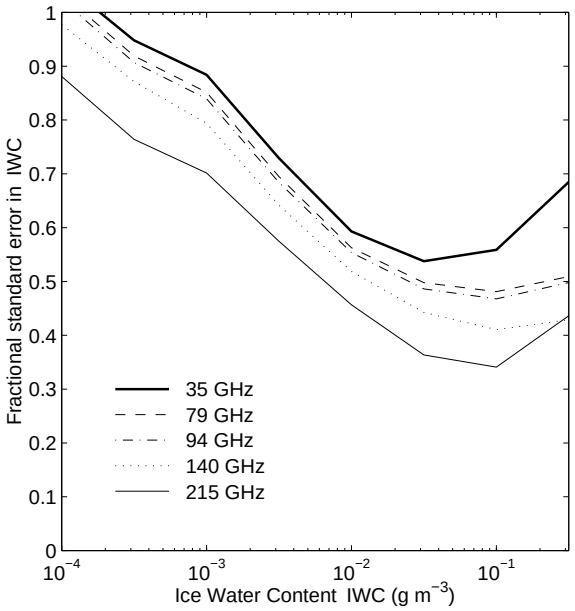


FIG. 4: Error in ice water content estimated by radar reflectivity at five frequencies for the EUCREX and CEPEX datasets, using best fits calculated from the two datasets combined.

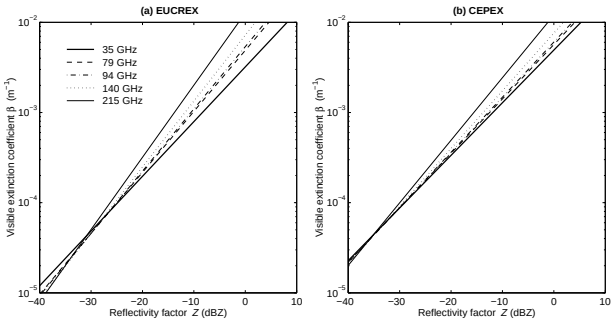


FIG. 5: The regression lines relating $Z$ to $\log_{10}(\beta)$ calculated from the coefficients in Table 2

diameter-dependence which is closer to that of IWC. The increase in fractional error at large IWC for the EUCREX case is partly a statistical effect due to the low number of samples; only 0.8% of the dataset had an IWC greater than 0.2 g m$^{-3}$. This is clearly apparent in Fig. 2.

The errors are due to variations in the mean size and the shape of the distribution, but do not include the effect of variations in density function, since it is very difficult to measure the density of individual crystals from aircraft.

Since the distinction between tropical and mid-latitude cirrus is somewhat artificial, it is conceivable that using the wrong set of fits on a particular observed cloud could significantly increase the error. We therefore combined the two datasets and recalculated the errors in IWC. The results are plotted in Fig. 4. It would appear that the tropical and mid-latitude datasets are sufficiently similar that the use of a single $Z$-IWC relationship for all points on the globe does not lead to a significant loss of accuracy.

Visible extinction coefficient $\beta_{\rm vis}$, defined in (2), can be more confidently calculated than IWC from aircraft size spectra alone because no assumption of density is required. However it was suggested by Arnott et al. (1994) that a sizeable number of crystals too small to be detected by the 2DC probe may contribute significantly to the extinction. More recent studies using a variety of instruments capable of measuring down to 5 $\mu$m (Mitchell et al. 1996; Kinne et al. 1997; McFarquhar and Heymsfield 1997) suggest that crystals smaller than 25 $\mu$m rarely dominate IWC or the radiative properties of cirrus.

Exactly the same procedure was carried out for $\beta_{\rm vis}$ as for IWC. The regression parameters are listed in Table 2, and the lines of best fit they represent are plotted in Fig. 5. The fractional error in $\beta_{\rm vis}$ as a function of $\beta_{\rm vis}$ is plotted in Fig. 6. The errors are slightly larger than for IWC, but again the highest frequencies are most accurate. It would be useful to compare visible or infrared radiometer measurements with radar derived optical depth using $Z$–$\beta_{\rm vis}$ relationships, with a view to exploring the ways an array of passive instruments along side the radar could validate and enhance the information provided by the radar.

One should be aware that through the depth of a particular cloud the errors in IWC or $\beta_{\rm vis}$ are likely to be in

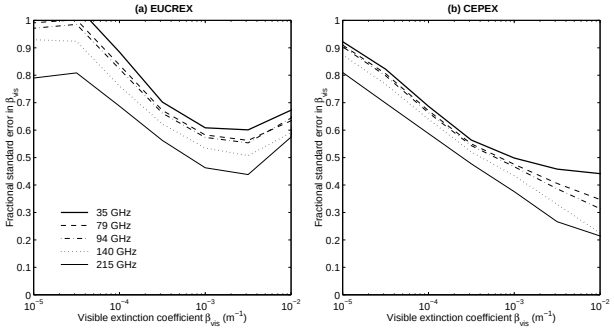


FIG. 6: Error in the visible extinction coefficient estimated from radar reflectivity at five frequencies for the EUCREX and CEPEX datasets.

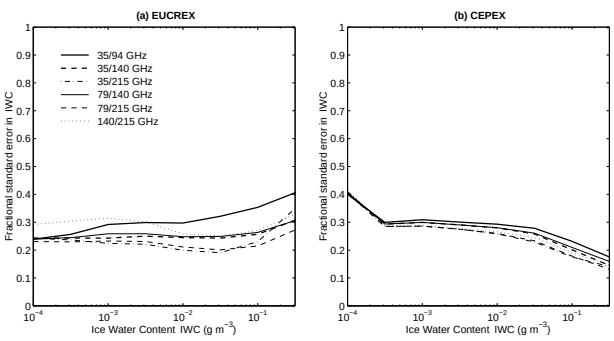


FIG. 7: Error in IWC estimated by dual-wavelength radar for six frequency combinations.

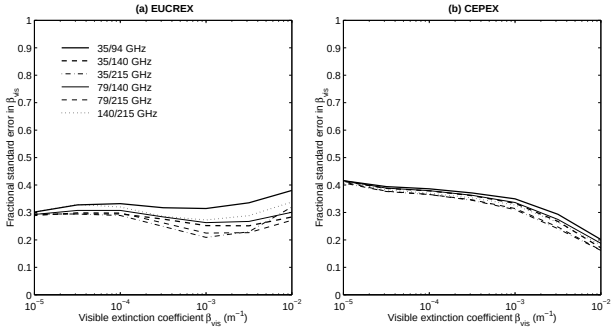


FIG. 8: Error in $\beta_{\rm vis}$ estimated by dual-wavelength radar.

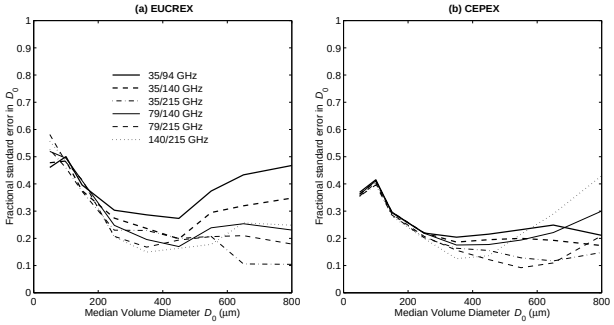


FIG. 9: Error in $D_0$ estimated by dual-wavelength radar.

the same sense, since the relationships between these parameters and $Z$ depend to some extent on the number concentration of ice nuclei. This can vary considerably but is likely to be correlated for a particular cloud. Hence vertically integrated quantities estimated from radar, such ice water path or optical depth, should be expected to have the same fractional error as IWC and $\beta_{\rm vis}$.

We conclude that if financial constraints were to restrict the satellite to carry only a single radar, then for estimating IWC and $\beta_{\rm vis}$ in cirrus, the highest frequencies are the best, although a judgement must be made as to whether attenuation by water vapor is too high at 140 and 215 GHz for these frequencies to be used if the detection of low clouds is also a priority.

### c. *Accuracy of dual-wavelength measurements*

Next we considered six dual-frequency combinations: 35/94, 35/140, 35/215, 79/140, 79/215 and 140/215 GHz. Firstly the accuracy of IWC was calculated assuming that DWR is known exactly, which would be the case for a radar with an infinite dwell time. The procedure was to calculate a best fit relating DWR to the ratio $g = {\rm IWC}/Z_{\rm low}$ and then to compare the true IWC with that given by $g \times Z_{\rm low}$, with $g$ derived from DWR using the best fit. The fit was calculated in log-log space since the best fit between log(DWR) and log($g$) is close to a straight line. The results are plotted in Fig. 7 and show considerable improvement over the single wavelength estimates. Essentially these findings are equivalent to those of Brown et al. (1995) for when some measure of mean size was known exactly. There is little difference between the various frequency combinations, although the 35/215 and 79/215 combinations exhibit slightly more accuracy. The remaining error of around 25–30% is due solely to the variation of the shape of the size distribution, and would be present for any technique which intrinsically assumes that one parameter (in this case $D_0$) is sufficient to describe distribution shape. Improvements beyond this should only be possible with some path constraint provided by radiometers.

The same procedure was repeated for $\beta_{\rm vis}$, and the results are plotted in Fig. 8. Again the error is a little higher than that for IWC. The error in measuring $D_0$ from DWR is shown in Fig. 9. Note that only 0.5% of the EUCREX data and 0.1% of the CEPEX data had $D_0$ greater than 800 $\mu$m.

### d. *Dual-wavelength measurements with realistic radar sensitivities*

The next step was to consider the effect of minimum sensitivities of $-30$ and $-40$ dBZ on the accuracy of DWR and on quantities derived from it. Normally-distributed random noise with a standard deviation cal-

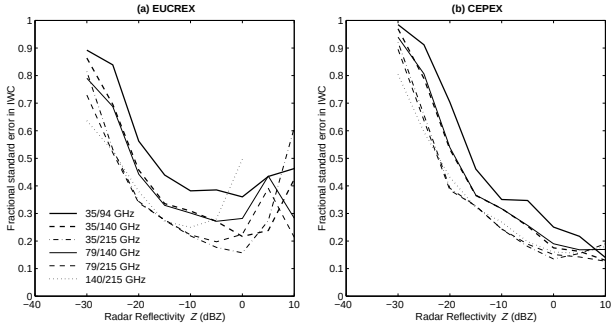


FIG. 10: Error in IWC derived from spaceborne dual-wavelength radar as a function of the reflectivity at the lower frequency, for a minimum detectable reflectivity of −30 dBZ.

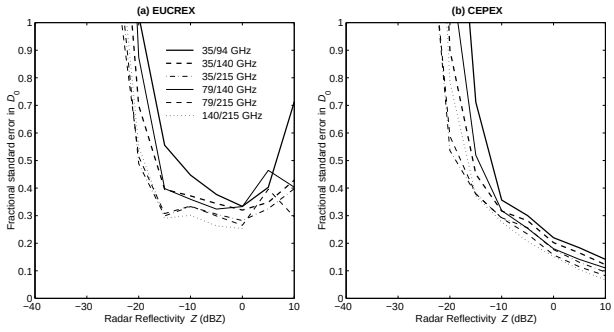


FIG. 11: Error in $D_0$ as a function of the reflectivity at the lower frequency, for a minimum detectable reflectivity of −30 dBZ.

culated from (9) and (11) was added to DWR (assuming that both frequencies had the same minimum detectable reflectivity) and the errors in IWC and $D_0$ were recalculated. In reality of course the higher frequencies would probably be more sensitive, but for dual-wavelength radar the least sensitive radar of the two is the determining factor for the accuracy of DWR.

A retrieval algorithm for a dual-wavelength radar needs to know the accuracy to which it can measure DWR and from this define a minimum value of DWR for sizing (as a function of $Z_{\text{low}}$ and $Z_{\text{high}}$) such that any values measured below this are deemed too inaccurate for size estimation and are rejected. Following Hogan et al. (2000) we set this limit to be twice the standard deviation of DWR; i.e. DWR $> 2\,\Delta$DWR.

Figure 10 shows the error in IWC as a function of the reflectivity of the lowest frequency radar of the pair, for a minimum reflectivity of −30 dBZ. The error for reflectivities of between −30 and −20 dBZ is large and only slightly better than the estimate for a single wavelength radar. Above −20 dBZ the most effective frequency combinations are clearly 35/215 and 79/215. The same for $D_0$ is shown in Fig. 11. One should be aware that in the lowest 10 dB of detectability some of the error is systematic, because by rejecting low values of DWR which fail the DWR $> 2\,\Delta$DWR criterion, we are only accepting

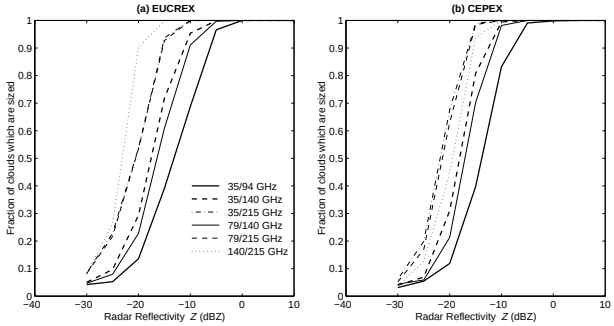


FIG. 12: The fraction of detected cloud at a given frequency that can be sized, for a minimum detectable reflectivity of -30 dBZ.

those pixels for which the random fluctuations happened to produce a larger DWR. Hence the measured size will usually be an overestimate. There is therefore a case for not estimating size when $Z_{\text{low}} < -20$ dBZ.

Figure 12 shows the fraction of detected cloud at a given reflectivity that can be sized. In the EUCREX data the 140/215 combination was best, being able to make size measurements in 90% of detected clouds with a reflectivity of −20 dBZ, whereas the value was only 10% for 35/94. For CEPEX the 35/215 and 79/215 combinations were able to measure size in the largest fraction of clouds. Dual-wavelength systems which include a 215 GHz radar are clearly the best both for accuracy and the fraction of clouds which can be sized, simply because at small sizes DWR is so much larger.

Figures 13–15 show the same as Figs. 10–12 but with a minimum detectable reflectivity of −40 dB. Again reliable size measurements are not possible in the lowest 10 to 20 dB of sensitivity, but the advantages of the higher sensitivity in faint clouds are apparent. Even if the sensitivity of the radars was somehow improved dramatically, if still only 2830 pulses were being averaged at each frequency then DWR would still have an intrinsic uncertainty of 0.12 dB and a lower limit for size measurement would remain. Meneghini and Kozu (1990) discussed a number of techniques for increasing the number of independent pulses $M_{\text{I}}$. A popular choice for a spaceborne radar is pulse compression, where conventional high-power, short-duration pulses are replaced by long coded pulses of low peak power, and frequency agility is also a possible means of increasing $M_{\text{I}}$.

## 4. Attenuation

### *a. Atmospheric gases*

Radars at frequencies higher than 94 GHz are generally considered to be unsuitable for ground-based observations of cirrus because of the strong water-vapor and oxygen absorption in the boundary layer. From space attenuation is far less of a problem. The nadir two-way gaseous attenuation from space has been calculated us-

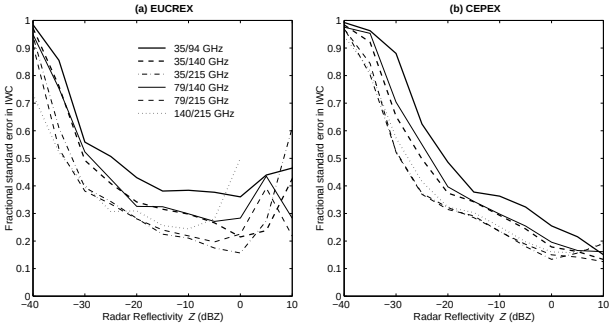


FIG. 13: Error in IWC derived from spaceborne dual-wavelength radar as a function of the reflectivity at the lower frequency, for a minimum detectable reflectivity of −40 dBZ.

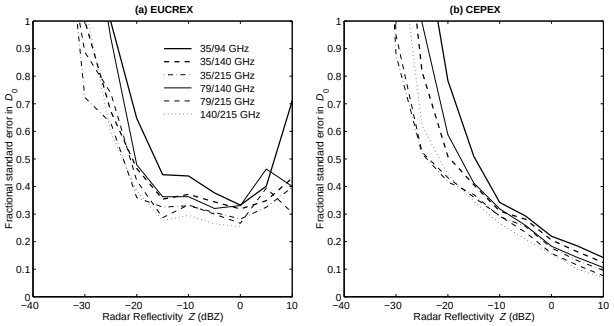


FIG. 14: Error in $D_0$ as a function of the reflectivity at the lower frequency, for a minimum detectable reflectivity of −40 dBZ.

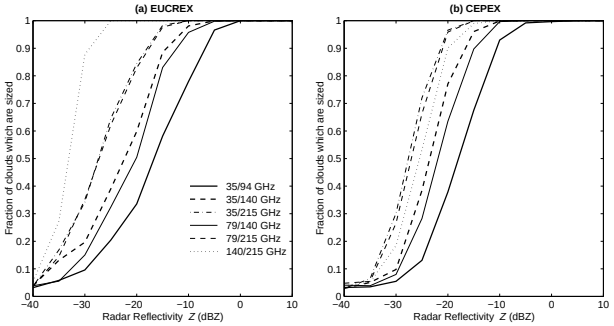


FIG. 15: The fraction of detected cloud at a given frequency that can be sized, for a minimum detectable reflectivity of -40 dBZ.

ing the line-by-line model of Liebe (1985), for a number of standard atmospheres taken from McClatchey et al. (1972), with saturated layers added at altitudes typical of cirrus. Figure 16 shows the profiles of temperature, relative humidity and the corresponding two-way nadir attenuation at each of the five frequencies, for the two most attenuating atmospheres (mid-latitude summer and tropical). It can be seen that the attenuation at 4 km/0°C reaches at most 0.8 dB at 140 GHz and 2 dB at 215 GHz. This is not a great problem for a dual-wavelength system with one frequency above 94 GHz and one at or below 94 GHz, since the reflectivity at the higher frequency can

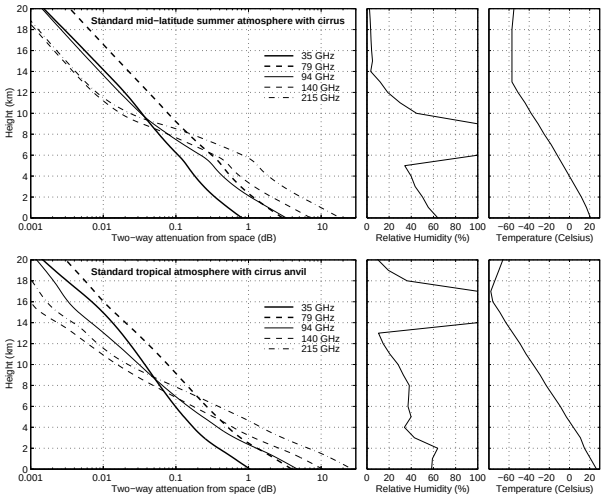


FIG. 16: The two-way attenuation from space at the frequencies 35, 79, 94, 140 and 215 GHz for two standard atmospheres with cirrus layers added at appropriate altitudes. The temperature and relative humidity profiles are shown to the right.

be matched with the less-attenuated lower frequency radar in the Rayleigh-scattering cloud top. Then attenuation can be corrected through the remainder of the cloud since it is reasonable to assume that the relative humidity is 100% where there is a cloud echo, and temperature is generally diagnosed well by global forecast models. Supposing after attenuation correction a 1 dB error in DWR remained just above the melting layer, then for a 79/215 GHz system this is not disastrous, representing only a 15% error in $D_0$ provided $D_0 > 500\,\mu$m at this point. It is apparent that the temperature of the cloud is very important; the mid-latitude cirrus layer at around −25°C in Fig. 16 is much more attenuating than the tropical anvil cirrus at −70°C because the saturation vapor pressure is so much higher at higher temperatures.

As well as monitoring ice clouds, a spaceborne radar is likely to also be employed for the detection of low-level clouds. The attenuation to the surface is considerable at 140 and 215 GHz in humid atmospheres and is unlikely to be fully offset by increased sensitivity due to the higher frequency. One of the three lower frequencies (35, 79 or 94 GHz) would probably be most suitable for the detection of low-level liquid water clouds, and it is doubtful that any useful additional information could be extracted from a second radar. The possibility of errors in the correction for attenuation is not a major concern because reflectivity is not well correlated with liquid water content or any property of low clouds that one might wish to measure (Fox and Illingworth 1997).

### *b. Ice crystals*

Attenuation by the ice crystals themselves is much smaller than that for liquid water with the same water

content, but increases sharply with frequency. We have calculated the extinction of the radar beam at each frequency from Mie theory for the EUCREX and CEPEX data, and Fig. 17 shows scatterplots of the two-way extinction against reflectivity factor for the frequencies 79, 140 and 215 GHz. At 79 GHz it is small enough to be neglected. This is not necessarily the case at higher frequencies. At 140 GHz, 0.2% of the CEPEX and 0.07% of the EUCREX data have a two-way extinction of over 1 dB km$^{-1}$. The respective values are 2.1% and 0.2% at 215 GHz. One should bear in mind that these high values are likely to be at cloud base, and the magnitude of DWR due to Mie scattering is likely to be much larger than any introduced by differential attenuation in ice. Extinction by ice crystals increases with ice density so these calculations are dependent on (4) being correct.

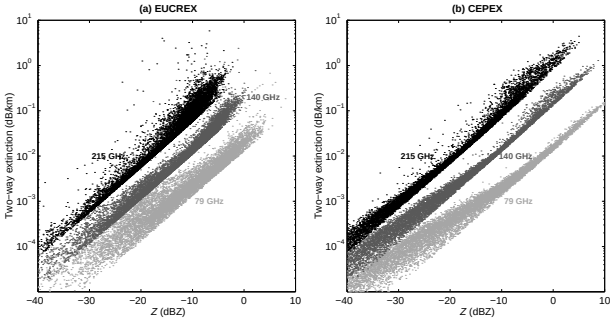


FIG. 17: Scatterplot of two-way ice crystal attenuation versus reflectivity at 79, 140 and 215 GHz, for the EUCREX and CEPEX datasets.

## 5. The effect of antenna configuration

### *a. Errors in DWR due to beamwidth differences*

To minimise instrumental bulk and ensure that the midpoints of the radar beams are very close it is probable that both frequencies of a spaceborne dual-wavelength system would use the same antenna. Previous work has considered a spaceborne cloud radar with an antenna diameter of around 2 m, which corresponds to a 1 km footprint from nadir at 94 GHz. The same antenna at 35, 79, 140 and 215 GHz would yield footprints of 2.69, 1.19, 0.67 and 0.44 km respectively. An important question is whether cloud inhomogeneities could cause random errors in DWR which would overwhelm those due to Mie scattering. Other alternatives exist however; the higher frequency radar could be defocussed, or constructed so that it under-illuminates the antenna. In this way the beams could be configured to match almost exactly, although at the cost of sensitivity at the higher frequency. From the radar equation we see that for a given transmit power the gain is proportional to the area of the antenna illuminated. Therefore if radars at the frequencies 79, 94, 140 and 215 GHz were to under-illuminate the antenna such that the resulting footprint matched that of a 35 GHz radar, then the losses in sensitivity would be 7.08, 8.60, 12.08 and 15.72 dB respectively. The same values would be applicable if the higher frequency radar was defocussed instead. These losses are large and so defocussing or under-illumination would only be considered if the alternative was unacceptably large errors in DWR.

It is necessary to estimate the magnitude of these errors using knowledge of the typical spatial structure of real cirrus clouds. This information has been obtained using vertically-pointing ground-based 35 and 94 GHz observations from the radar facility at Chilbolton, England taken between June and September 1996. Ten second averages of reflectivity factor were recorded with a vertical resolution of 75 m. Averaging was performed to reduce the vertical resolution to 525 m, close to the 500 m proposed for a spaceborne radar. A number of 1024-point time-series of reflectivity factor (in dBZ) in cirrus were selected, and the temporal scale converted to a spatial scale using a simple Taylor transformation and the mean wind speed over Chilbolton at that time and altitude as diagnosed by the UK Meteorological Office Unified Model. Only time-series in which all points registered cloud were considered. Information on the horizontal structure was then obtained by fitting power laws of the form

$$E = E_0 k^{\mu} \tag{12}$$

to the Fourier spectra of these data, where $k$ is wavenumber, $E$ is power spectral density, and $E_0$ and $\mu$ are constants. The best fit lines were least squares fits in log-log space after 7-point averaging of the spectra to reduce scatter. The parameter $\mu$ was found to vary between $-1.8$ and $-2.4$ in cirrus, which compares with the range $-1$ to $-2$ found by Danne et al. (1996). A spectrum typical of those we analysed was obtained on 22 June 1996 and is shown in Fig. 18. It had the form $E = 2.03 \times 10^{-5} k^{-2.16}$ dBZ$^2$ m (where $k$ is in m$^{-1}$), and we will use this from now on.

The next step was to determine the difference in reflectivity due to different footprints, by simulating two-dimensional cloud fields from the one-dimensional spectral information. This could have been done analytically but for the mathematical complication that useful spectra can only be calculated from reflectivity in logarithmic units, whereas averaging must be performed on reflectivity in linear units. Cloud fields were generated by calculating the inverse two-dimensional Fourier transform of synthetic matrices containing wave amplitudes consistent with the energy at the various scales indicated by the one-dimensional spectrum. The phase of each wave component of the matrix was random, so that each cloud field was different. The domains were square and measured 15.36 km on a side with a resolution of 120 m. Fourier analysis of cross-sections through the domain confirmed that they had almost identical spectral properties as the original data. An example is shown in Fig. 19. Note that these cloud fields are spectrally isotropic, whereas

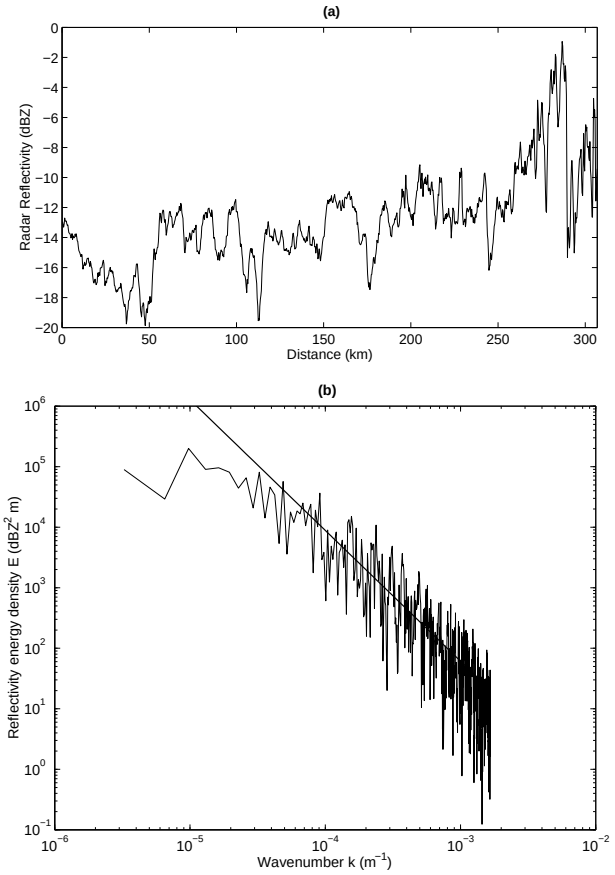


FIG. 18: (a) 35 GHz reflectivity factor at an altitude of 7 km, measured from Chilbolton on 22 June 1996. The abscissa has been converted from time to space using a mean wind at this altitude of 30 m s$^{-1}$. (b) The corresponding power spectrum. The best fit line is $E = 2.03 \times 10^{-5} k^{-2.16}$.

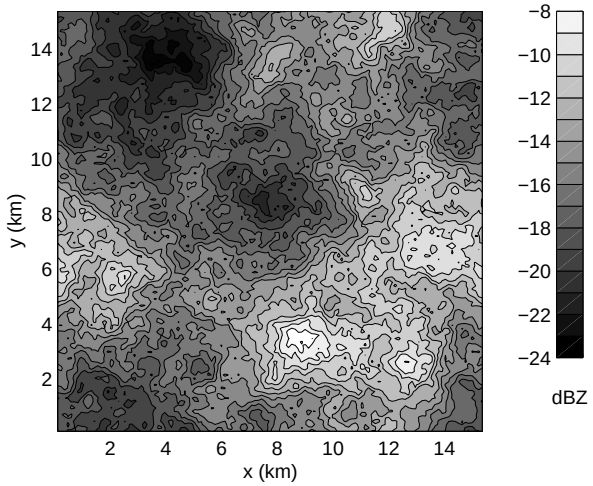


FIG. 19: Example of a simulated two-dimensional cloud field.

real cirrus clouds with fallstreaks are not because the fallstreaks tend to be aligned parallel to the vertical wind-shear vector. On average this is not expected to significantly bias the results.

| Dual-wavelength frequencies | Error in DWR (dB) |
|---|---|
| 35/94 | 0.21 |
| 35/140 | 0.25 |
| 35/215 | 0.27 |
| 79/140 | 0.067 |
| 79/215 | 0.097 |
| 140/215 | 0.031 |

TABLE 3: The error in DWR due to different beamwidths.

Following Illingworth et al. (1997), we shall consider a 1 second averaging time for the radar to achieve sufficient sensitivity, which results in a pixel length of 7 km. The beam patterns are assumed to be Gaussian. The standard deviation of DWR due only to differing beamwidths has been calculated for each frequency combination from 64 simulated cloud fields; these are listed in Table 3. Clearly the error is reduced for the shorter wavelength pairings because cloud reflectivity fluctuates less at smaller scales. These values need to be put into perspective by comparing with the typical magnitudes of DWR which occur in cirrus, as shown in Fig. 1. For the three frequency combinations which do not include 35 GHz, the error in DWR is less than 0.1 dB which is less than the minimum error in DWR due to averaging over only 2830 pulses (0.12 dB). For combinations which include 35 GHz, it is over 0.2 dB and so could reduce the accuracy of size measurements at small sizes. In any case these errors are not really large enough to consider defocussing or under-illumination as a worthwhile option for the higher frequency radar. This is in contrast to the use of dual-wavelength radar for hail detection (e.g. Atlas and Ludlam 1961); it was found by Rinehart and Tuttle (1982) that reflectivity gradients of the order of 20 dB km$^{-1}$ at the edge of convective storms could produce anomalous values of DWR due to differences in the side-lobe level, even if the main lobes were well matched. However, gradients of this magnitude are never observed in cirrus.

A further problem with using the same parabolic antenna for two frequencies is that both sources cannot be placed precisely on the focal line, so the beam pattern is somewhat degraded and there is an increase in the level of the first few sidelobes (Meneghini and Kozu 1990).

### *b. Errors in* DWR *caused by non-coincident footprints*

It has been suggested that financial constraints may exclude the possibility of a payload of two active instruments on a cloud profiling satellite, and that work should be carried out to determine whether or not dividing the instruments between two satellites in very close orbits would severely reduce the accuracy of size retrievals. It has been shown that a second satellite could at best trail the first by 5 minutes, with the footprints drifting towards

and away from each other by as much as 5 km. The effect of this has been simulated using cloud fields with a resolution of 500 m and measuring 64 × 64 km. The swaths of two spaceborne radars, each with a footprint of 1 km and a 7 km pixel length, were offset by up to 10 km in the directions both parallel and perpendicular to the satellite motion. Figure 20 shows the error in DWR as a function of separation distance in both directions. A 5 km offset of the footprints perpendicular to the direction of motion of the satellite results in an error in DWR of between 2 and 2.5 dB. For a wind speed of 30 $m\,s^{-1}$, 5 minutes corresponds to 9 km, so the reflectivity measured by two satellites in the same orbit but 5 minutes apart could differ by as much as 3.5 dB. It has been assumed that advection is much more important than cloud evolution over these timescales, but cloud development could in theory introduce more error.

We conclude that for dual-wavelength radar at least, there little point in even attempting to derive size with errors of this magnitude, and the same is probably true of radar/lidar synergy. It would in fact be better for two separate satellite-borne radars to be in completely different orbits to obtain a better global coverage.

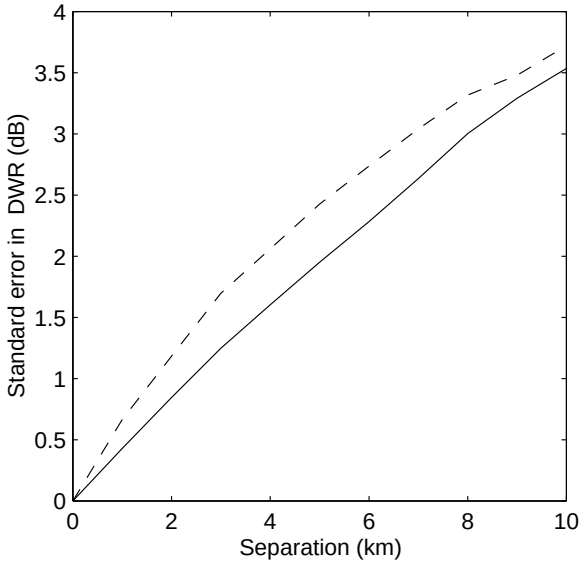


FIG. 20: The standard error in DWR as a function of swath separation for radars mounted separately on two satellites. The solid line is for swaths separated in the direction parallel to the direction of motion of the satellites (satellites in the same orbit but one lagging the other), and the dashed line is for swaths separated in the direction perpendicular to the direction of motion (satellites in adjacent orbits).

## 6. Other considerations

### *a. Crystal habit*

So far we have considered only a nadir pointing radar viewing spherical ice crystals. A problem arises however because non-spherical crystals tend to fall with their longest axis aligned horizontally (although the azimuthal orientation is random), and the magnitude of DWR in fact depends on the dimension of the crystals in the direction parallel to the direction of propagation of the incident radiation. In consequence the median *equivolumetric* diameter $D_0$, which we need to measure, is underestimated by nadir or zenith pointing dual-wavelength radars if the reflectivity of the cloud is dominated by the contribution from non-spherical crystals.

A straightforward solution is to view at an angle of 45° from nadir, which results in DWR being much more closely related to equivolumetric diameter, and the spherical approximation can be used much more confidently. Figure 21 shows DWR versus $D_0$ for horizontally-aligned oblate crystals with various aspect ratios, as viewed by each of the six wavelength combinations both from nadir and at 45° from nadir. These were calculated using the T-matrix method (Waterman 1969) for an exponential size distribution. It would appear that if the crystals which dominate the reflectivity are significantly aspherical then viewing from nadir could result in a serious underestimate of crystal size; to a first approximation when the aspect ratio is 0.5, say, then for a given $D_0$ the dual-wavelength ratio will be 0.5 of its value for a sphere. This problem is found to be almost eliminated by viewing at 45°, and calculations for prolate crystals produce similar results. The presence of canting crystals should not really be a problem since on average the dimension of the crystal measured by the radars should still be close to $D_0$. The obvious drawback of the alternative viewing angle is that attenuation is increased by a factor of $\sqrt{2}$, and the greater distance from the satellite to the cloud would further reduce the sensitivity by 3 dB.

### *b. Calibration*

Any gains in the accuracy of IWC by the use of two radars are lost if the absolute calibration of the radars cannot be determined better than the intrinsic accuracy of the technique itself. The minimum error in IWC is around 15% with the dual-wavelength method (see Figs. 10 and 13), so the radars need be calibrated to within 0.5 dB. In theory the return from the ocean could provide a useful high-reflectivity means of regular calibration. However the backscatter from the sea depends on the amplitude of surface waves with a wavelength of the order of the wavelength of the radar, and errors in determining this may exceed 0.5 dB. Water vapor attenuation at the higher frequencies may also be difficult to account for exactly. Calibration campaigns with aircraft and ground based radars would almost certainly prove necessary.

The relative calibration of the radars is less of a problem; Hogan et al. (2000) were able to match the reflectivities measured by the two radars of a dual-wavelength system in the Rayleigh-scattering cloud top. Unfortunately

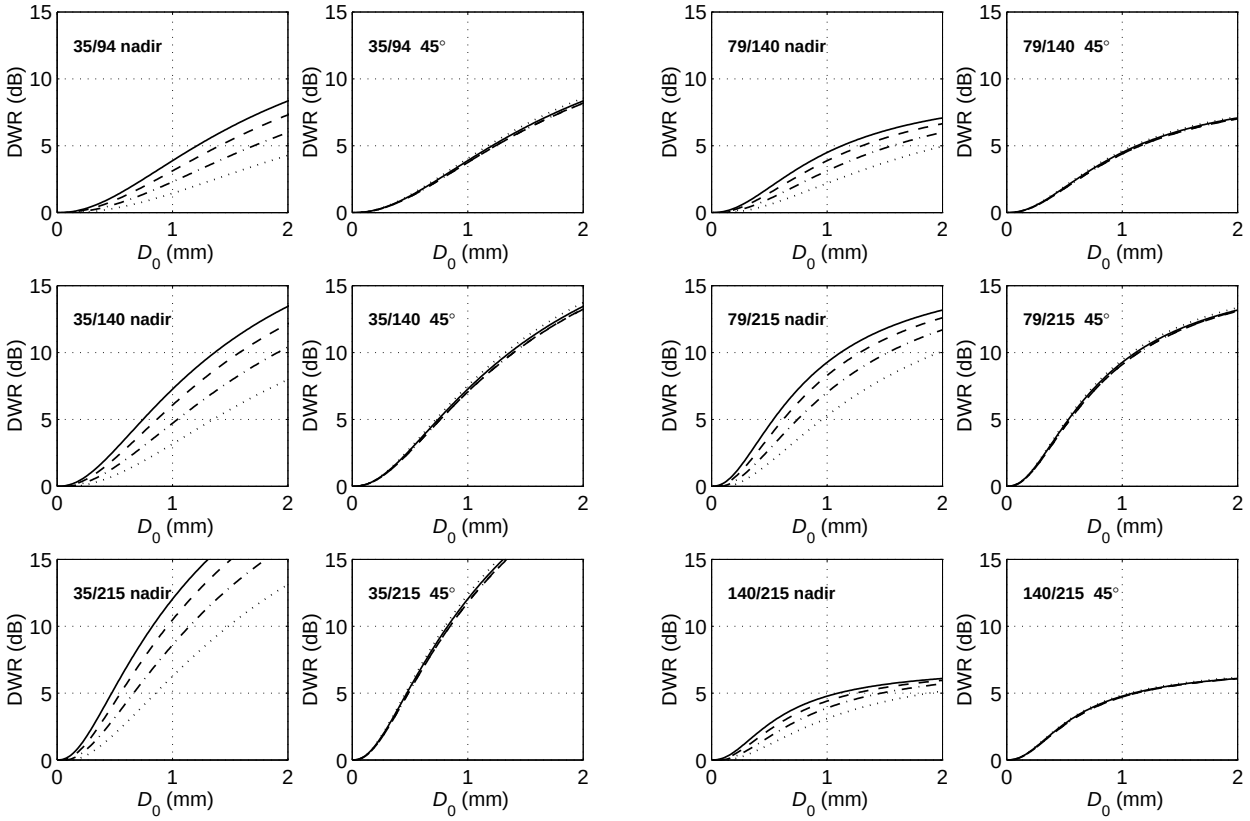


FIG. 21: Dual-wavelength ratio DWR as a function of median volume diameter $D_0$ for six frequency combinations. The crystals are horizontally aligned and oblate, with four different aspect ratios: 1 (solid line), 0.8 (dashed line), 0.6 (dot-dashed line) and 0.4 (dotted line). The results for both nadir and 45° from nadir are shown, and the size distributions are exponential.

this is generally the region of the cloud with lowest reflectivity, so the radars must be sufficiently sensitive that the precision of $Z$ here is still high. This is especially true when one of the radars is at 215 GHz, since for the reflectivities to be matched to within 0.1 dB, $D_0$ must be less than around 70 $\mu$m, compared with 150 $\mu$m for the 35/94 combination.

## 7. Conclusions

We have explored the feasibility of spaceborne single and dual-wavelength radar, at a range of frequencies, for the global measurement of ice water content, visible extinction coefficient and crystal size in cirrus.

Firstly the accuracy of single wavelength estimates of IWC and $\beta_{\rm vis}$ were calculated from EUCREX and CEPEX data for the wavelengths 35, 79, 94, 140 and 215 GHz. Results for 94 GHz were in agreement with those of Brown et al. (1995), but because of increased Mie scattering at higher frequencies, at 140 GHz the errors were reduced by up to 5% compared with 94 GHz, and at 215 GHz by between 10 and 20%. Two-way gaseous attenuation is shown to be unlikely to significantly bias the results, since even at 215 GHz it would typically reach only 2 dB at the melting level for a nadir-viewing radar, which could be corrected for with reasonable accuracy. Attenuation by ice crystals was found to exceed 1 dB km$^{-1}$ at 215 GHz in 2.1% of the CEPEX and 0.8% of the EUCREX data, which is less easy to correct for but does not represent a significant bias given the inherent errors in the $Z$–IWC and $Z$–$\beta_{\rm vis}$ relationships. We conclude that if only cirrus clouds are of interest then a 215 GHz radar would be the preferred choice, but if the detection of low level clouds is also a requirement then to minimise attenuation, 79 or 94 GHz should be used.

The next step was to consider a spaceborne dual-wavelength radar that could measure DWR exactly. In this case the errors in IWC and $\beta_{\rm vis}$ were mostly in the range 25–35% and varied little depending on which frequency combination was used. These errors are due to variations in the shape of the distribution and represent the greatest achievable accuracy of the dual-wavelength technique. For $D_0 > 250$ $\mu$m, the error in $D_0$ ranged between 15 and 25% when the higher frequency of the two radars was 215 GHz, and between 20 and 40% otherwise. Diameter measurements at smaller sizes were less accurate, especially in the EUCREX data.

We then considered the accuracy achievable by radars with minimum sensitivities of −30 and −40 dBZ, and a dwell time of 1 second. At reflectivities over 20 dB more than the minimum reflectivity, errors in IWC and $D_0$ were nearly always less than 30% when the highest frequency was 215 GHz, and less than 40% when the highest frequency was 140 GHz. In the lowest 15–20 dB of sensitivity, random errors in DWR were large enough and average crystal size small enough that dual-wavelength measurements were little better than those from a single wavelength radar. Frequency combinations which included 215 GHz were able to measure size in a much greater fraction of clouds at low signal-to-noise ratio.

The weakness of this technique is clearly in low reflectivity clouds containing only small crystals, where a lidar and radar or multiple wavelength lidar would probably be more accurate. In thicker more radiatively significant cloud the dual-wavelength radar method is relatively accurate, while lidar would begin to experience appreciable attenuation and multiple scattering. As stated by Brown and Francis (1995), there is a need to validate the algorithm to determine radar reflectivity from aircraft data.

The possibility of errors in DWR from a number of other sources was considered. These should be compared with the intrinsic minimum error of 0.12 dB due to a dwell time of 1 second, and the magnitudes of DWR that we wish to measure, indicated in Fig. 1. The error due to beamwidth differences was found to be typically between 0.2 and 0.3 dB for frequency combinations which included 35 GHz, and between 0.03 and 0.1 dB otherwise. Mounting the two radars on different satellites was found to introduce an error of at least several decibels, which is far too great for such a scenario to ever be considered seriously. A nadir pointing dual-wavelength radar would be sensitive to crystal shape, but we present evidence from scattering calculations which suggests that if the crystals were aligned with their longest axis in the horizontal, then viewing at an angle of 45° from nadir should virtually eliminate the problem.

We conclude that the combination of 79 and 215 GHz at a viewing angle of 45° from nadir would be the best configuration for observing cirrus clouds.

## Acknowledgements

We are grateful to Philip R. A. Brown for providing the EUCREX data, and to Andrew J. Heymsfield for the CEPEX data. Thanks are also due to the Rutherford Appleton Laboratory for providing the Chilbolton radar data. The observational studies were funded by NERC grant GR3/8765, and the first author is funded by a NERC studentship.

## REFERENCES

Arnott, W. P., Y. Y. Dong and J. Hallett, 1994: Role of small ice-crystals in radiative properties of cirrus: A case study, Fire II 22 Nov 1991. *J. Geophys. Res.*, **99**, 1371–1381.

Atlas, D., and F. H. Ludlam, 1961: Multi-wavelength radar reflectivity of hailstorms. *Quart. J. Roy. Meteor. Soc.*, **87**, 523–534.

Atlas, D., S. Y. Matrosov, A. J. Heymsfield, M.-D. Chou and D. B. Wolff, 1995: Radar and radiation properties of ice clouds. *J. Appl. Meteor.*, **34**(11), 2329–2345.

Brown, P. R. A., 1993: Measurement of the ice water content of cirrus using an evaporative technique. *J. Atmos. Oceanic Technol.*, **10**, 579–590.

Brown, P. R. A., and P. N. Francis, 1995: Improved measurements of the ice water content in cirrus using a total-water probe. *J. Atmos. Oceanic Technol.*, **12**(2), 410–414.

Brown, P. R. A., A. J. Illingworth, A. J. Heymsfield, G. M. McFarquhar, K. A. Browning and M. Gosset, 1995: The role of spaceborne millimeter-wave radar in the global monitoring of ice-cloud. *J. Appl. Meteor.*, **34**(11), 2346–2366.

Danne, O., G. G. Mace, E. E. Clothiaux, X. Dong, T. P. Ackerman and M. Quante, 1996: Observing structures and vertical motions within stratiform clouds using a vertical pointing 94-GHz cloud radar. *Beitr. Phys. Atmosph.*, **69**(1), 229–237.

Doviak, R. J., and D. S. Zrnić, 1993: *Doppler radar and weather observations*. 2nd Ed. Academic Press.

Fox, N. I., and A. J. Illingworth, 1997: The potential of a spaceborne radar for the detection of stratocumulus clouds. *J. Appl. Meteor.*, **36**(6), 676–687.

Hogan, R. J., A. J. Illingworth and H. Sauvageot, 2000: Measuring crystal size in cirrus using 35- and 94-GHz radars. *J. Atmos. Oceanic Technol.*, **17**(1), 27–37.

Illingworth, A. J., C. Liu, I. Astin and B. Richards, 1997: *Study of the critical requirements for a cloud radar.* Final report, ESTEC Contract 11346/95/NL/CN.

Intrieri, J. M., G. L. Stephens, W. L. Eberhart and T. Uttal, 1993: A method for determining cirrus cloud particle sizes using lidar and radar backscatter techniques. *J. Appl. Meteor.*, **32**(6), 1074–1082.

Kinne, S., T. P. Ackerman, M. Shiobara, A. Uchiyama, A. J. Heymsfield, L. Miloshevich, J. Wendell, E. W. Eloranta, C. Purgold and R. W. Bergstrom, 1997: Cirrus cloud radiative and microphysical properties from ground observations and in situ measurements during FIRE 1991 and their application to exhibit problems in cirrus solar radiative transfer modeling. *J. Atmos. Sci.*, **54**, 2320–2344.

Lhermitte, R. M., 1988: Observation of rain at vertical incidence with a 94 GHz Doppler radar—and insight on Mie scattering. *Geophys. Res. Lett.*, **15**(10), 1125–1128.

Liebe, H. J., 1985: An updated model for millimeter-wave propagation in moist air. *Radio Science*, **20**(5), 1069–1089.

Liebe, H. J., T. Manabe and G. A. Hufford, 1989: Millimeter-wave attenuation and delay rates due to fog/cloud conditions. *IEEE AP*, **37**, 1617–1623.

Matrosov, S. Y., 1993: Possibilities of cirrus particle sizing from dual-frequency radar measurements. *J. Geophys. Res.*, **98**(D11), 20 675–20 683.

Maxwell-Garnet, J. C., 1904: Colours in metal glasses and metallic films. *Philos. Trans. Roy. Soc.*, **A203**, 385–420.

McClatchey, R. A., R. W. Fenn, J. E. A. Selby, F. E. Volz and J. S. Garing, 1972: Optical properties of the atmosphere (3rd. ed.), Air Force Cambridge Research Laboratories, Rep. No. AFCRL72-0497, L. G. Hanscom Field.

McFarquhar, G. M., and A. J. Heymsfield, 1997: Parameterization of tropical cirrus ice crystal size distributions and implications for radiative transfer: Results from CEPEX. *J. Atmos. Sci.*, **54**, 2187–2200.

Mead, J. B., R. E. McIntosh, D. Vandemark and C. T. Swift, 1989: Remote sensing of clouds and fog with a 1.4-mm radar. *J. Atmos. Oceanic Technol.*, **6**, 1090–1097.

Meneghini, R., and T. Kozu, 1990: *Spaceborne weather radar.* Artech House.

Meneghini, R., and L. Liao, 1996: Comparisons of cross-sections for melting hydrometeors as derived from dielectric mixing formulas and a numerical-method. *J. Appl. Meteor.,* **35**(10), 1658–1670.

Mitchell, D. L., S. K. Chai, Y. Liu, A. J. Heymsfield and Y. Dong, 1996: Modeling cirrus clouds. 1: Treatment of bimodal size spectra and case study analysis. *J. Atmos. Sci.,* **53**(20), 2952–2966.

Rinehart, R. E., and J. D. Tuttle, 1982: Antenna beam patterns and dual-wavelength processing. *J. Appl. Meteor.,* **21**, 1865–1880.

Stephens, G. L., S. C. Tsay, P. W. Stackhouse Jr. and P. J. Flatau, 1990: The relevance of the microphysical and radiative properties of cirrus clouds to climate and climatic feedback. *J. Atmos. Sci.,* **47**, 1742–1752.

Waterman, P., 1969: Scattering by dielectric obstacles. *Alta Freq.,* **38**, 348–352.